

# Potential Drug Interactions Mediated by Renal Organic Anion Transporter OATP4C1<sup>§</sup>

Toshihiro Sato, Eikan Mishima, Nariyasu Mano, Takaaki Abe, and Hiroaki Yamaguchi

Department of Pharmaceutical Sciences, Tohoku University Hospital (T.S., N.M., H.Y.); Division of Nephrology, Endocrinology, and Vascular Medicine, Graduate School of Medicine (E.M., T.A.); Division of Medical Science, Graduate School of Biomedical Engineering (T.A.); Department of Clinical Biology and Hormonal Regulation, Graduate School of Medicine (T.A.), Tohoku University, Sendai, Japan

Received March 27, 2017; accepted May 24, 2017

## ABSTRACT

Organic anion-transporting polypeptide 4C1 (OATP4C1) is an organic anion transporter expressed in the basolateral membrane of the renal proximal tubules. It plays a major role in the urinary excretion of both exogenous drugs and endogenous compounds. Our previous studies have indicated the importance of OATP4C1 in pathologic and physiologic conditions; however, the majority of its pharmacologic characteristics remained unclear. Therefore, to provide essential information for clinical drug therapy decisions and drug development, we clarified drug interactions mediated by OATP4C1. To elucidate potential drug interactions via OATP4C1, we screened 53 representative drugs commonly used in clinical settings. Next, we evaluated the IC<sub>50</sub> values of drugs that inhibited OATP4C1 by more than 50%. To apply our results to clinical settings, we calculated the drug-drug interaction (DDI) indices.

The screening analysis using an OATP4C1-expressing cell system demonstrated that 22 out of 53 therapeutic drugs inhibited OATP4C1-mediated triiodothyronine transport. In particular, OATP4C1-mediated transport was strongly inhibited by 10 drugs. The IC<sub>50</sub> values of 10 drugs—nicardipine, spironolactone, fluvastatin, crizotinib, levofloxacin, clarithromycin, ritonavir, saquinavir, quinidine, and verapamil—obtained in this study were 51, 53, 41, 24, 420, 200, 8.5, 4.3, 100, and 110 μM, respectively. The IC<sub>50</sub> values of these drugs were higher than the plasma concentrations obtained in clinical practice. However, ritonavir showed the highest DDI index (1.9) for OATP4C1, suggesting that it may strongly influence this transporter and thus cause drug interactions seen in clinical settings. Our finding gives new insight into the role of OATP4C1 in clinical DDIs.

## Introduction

The kidney plays an important role in the excretion of endogenous and exogenous compounds by moving them from the blood into the urine. Urinary excretion involves two main processes: glomerular filtration and tubular secretion. Renal tubular secretion is mediated by membrane transporters expressed in the proximal tubules, including the organic anion-transporting polypeptide (OATP) family, organic anion transporter (OAT) family, organic cation transporter (OCT) family, multi-drug and toxic compound extrusion (MATE) family, and ATP-binding cassette (ABC) family.

The OATP family comprises sodium-independent organic anion transporters found in a variety of tissues, including the liver, kidney, intestines, and brain. OATP transporters contribute to the transport of bile acids, thyroid hormones, steroid conjugates, anionic oligopeptides, eicosanoids, various drugs, and

other xenobiotic compounds across membranes (Hagenbuch and Meier, 2003, 2004; Kullak-Ublick et al., 2004; Mikkaichi et al., 2004a; Sato et al., 2014, 2017; Suga et al., 2017).

OATP4C1 is the first member of the OATP family found to be predominantly expressed in the kidney. OATP4C1, which is localized in the basolateral membrane of the proximal tubule, plays a major role in the urinary secretion of cardiac glycosides (digoxin and ouabain), thyroid hormones (triiodothyronine [T<sub>3</sub>] and thyroxine), cAMP, methotrexate, sitagliptin, estrone 3-sulfate, chenodeoxycholic acid, and glycocholic acid (Mikkaichi et al., 2004b; Chu et al., 2007; Yamaguchi et al., 2010). Moreover, our previous study suggested that estrone 3-sulfate does not bind to the recognition site for digoxin in the OATP4C1 molecule (Yamaguchi et al., 2010). Toyohara et al. (2009) showed that overexpression of human *SLCO4C1*, which encodes OATP4C1 in a rat model of chronic kidney disease (CKD), ameliorated the progression of renal damage, hypertension, cardiomegaly, and inflammation by reducing the accumulation of uremic toxins such as guanidino succinate, asymmetric dimethylarginine, and *trans*-aconitate. However, the pharmacologic characteristics of OATP4C1 such as drug-drug interactions (DDIs) are not well studied. In the

This work was supported by grants from the Japan Society for the Promotion of Science KAKENHI [Grant 23790168 (to H.Y.) and 15H00485 (to T.S.)].

<https://doi.org/10.1124/jpet.117.241703>.

<sup>§</sup> This article has supplemental material available at [jpet.aspetjournals.org](http://jpet.aspetjournals.org).

**ABBREVIATIONS:** ABC, ATP-binding cassette; CKD, chronic kidney disease; CYP3A, cytochrome P450 isoform 3A; DDI, drug-drug interaction; ESI, electrospray ionization; FDA, U.S. Food and Drug Administration; KH buffer, Krebs-Henseleit buffer; LC/MS/MS, liquid chromatography with tandem mass spectrometry; MATE, multidrug and toxic compound extrusion; NGS, normal goat serum; OATP, organic anion-transporting polypeptide; OCT, organic cation transporter; PBS, phosphate-buffered saline; P-gp, P-glycoprotein; T<sub>3</sub>, triiodothyronine.

present study, to provide essential information for drug therapy and drug development, we clarified clinically relevant drug interactions via OATP4C1.

## Materials and Methods

**Materials.** We purchased T<sub>3</sub> and sodium butyrate from Nacalai Tesque (Kyoto, Japan). All other chemicals were commercially available and of the highest purity possible.

**Cell Culture and Establishment of OATP4C1 Stably Expressing Cells.** MDCKII cells were cultured in Dulbecco's modified Eagle's medium supplemented with 10% fetal bovine serum under an atmosphere of 5% CO<sub>2</sub> and 95% air at 37°C. The cells were transfected with a *pcDNA3.1(+)* plasmid vector (ThermoFisher Scientific, Waltham, MA) encoding OATP4C1 using Lipofectamine 3000 (ThermoFisher Scientific) according to the manufacturer's instructions. After 3 weeks of selection in G418 (0.5 mg/ml), we screened single colonies for OATP4C1 expression by transport studies. Cells transfected with the empty vector were used as controls.

**Western Blot Analysis.** Cells were lysed in radioimmunoprecipitation assay buffer (Santa Cruz Biotechnology, Santa Cruz, CA). The protein content of the solubilized cells was determined by the Bradford method using a Protein Assay kit (Bio-Rad Laboratories, Hercules, CA) with bovine serum albumin used as a standard. We subjected 50 µg of protein to SDS-PAGE and then transferred to Immobilon-P polyvinylidene fluoride membranes (Bio-Rad Laboratories). The blots were blocked by 5% skim milk in Tris-buffered saline (2 mM Tris, 138 mM NaCl, pH 7.6) containing 0.1% Tween 20 at room temperature for 30 minutes; they were then probed with anti-human SLC04C1 antibody (1:1000 dilution, HPA036516; Sigma-Aldrich, St. Louis, MO) at 4°C overnight. The blots were washed and then incubated with goat anti-rabbit IgG conjugated with horseradish peroxidase (1:1000 dilution; Pierce, Rockford, IL). The ECL Plus chemiluminescent system (GE Healthcare UK, Little Chalfont, United Kingdom) was used for detection.

**Immunohistochemistry.** Mock and OATP4C1-expressing MDCKII cells were fixed with 10% formaldehyde neutral buffer solution (Nacalai Tesque). After incubation in phosphate-buffered saline (PBS) containing 0.1% Triton-X100 at room temperature for 5 minutes, the specimens were blocked with 3% normal goat serum (NGS) in PBS at room temperature for 10 minutes, and then probed with anti-human SLC04C1 antibody (1:100 dilution) in PBS containing 3% NGS (HPA036516; Sigma-Aldrich) at 4°C overnight. The specimens were then incubated with CF594 F(ab')<sub>2</sub> fragment of goat anti-rabbit IgG (1:500 dilution; Biotium, Fremont, CA) in PBS containing 3% NGS at room temperature for 1 hour.

For immunofluorescent microscopy, cells were double stained with the nucleus marker 4',6-diamidino-2-phenylindole (DAPI). After washing with PBS and fixing by mounting medium, images were taken with a C2<sup>+</sup> laser confocal microscope system (Nikon Corporation, Tokyo, Japan).

**Transport Studies.** The cellular uptake in monolayer cultures grown on 24-well plates was measured. After washing once, the cells were preincubated in Krebs-Henseleit (KH) buffer (118 mM NaCl, 23.8 mM NaHCO<sub>3</sub>, 4.83 mM KCl, 0.96 mM KH<sub>2</sub>PO<sub>4</sub>, 1.20 mM MgSO<sub>4</sub>, 12.5 mM *N*-(2-hydroxyethyl) piperazine-*N'*-2-ethanesulphonic acid, 5.0 mM D-glucose, and 1.53 mM CaCl<sub>2</sub>, pH 7.4). Uptake was initiated by adding T<sub>3</sub> with or without any of the trial drugs. At the indicated times, uptake was terminated by replacing the uptake buffer with ice-cold KH buffer and then washing twice with ice-cold KH buffer. Concentration of T<sub>3</sub> was measured by liquid chromatography with tandem mass spectrometry (LC/MS-MS). The uptake was calculated by dividing the uptake amount by the protein amount of the cells.

**Inhibitory Effects of Various Therapeutic Drugs.** We calculated the IC<sub>50</sub> values of drugs that inhibited OATP4C1-mediated uptake of T<sub>3</sub> by over 50%. The IC<sub>50</sub> values were estimated using a

nonlinear least-squares regression analysis of the competition curves by use of eq. 1:

$$V = \frac{100 \times \text{IC}_{50}^n}{\text{IC}_{50}^n + [I]^n} \quad (1)$$

where  $V$  is the transport amount (% of control),  $[I]$  is the drug concentration, and  $n$  is the Hill coefficient.

**Drug-Drug Interaction Index Prediction.** To relate our findings to clinical applications, we calculated the DDI index (Ito et al., 1998; CDER, 2012; Izumi et al., 2015) according to the U.S. Food and Drug Administration (FDA) guidelines. We used the maximum plasma concentration ( $C_{\text{max}}$ ) and the maximum concentration of unbound drug in plasma ( $C_{\text{max,u}}$ ) for each drug and the IC<sub>50</sub> values from our *in vitro* study to predict the possibility of a clinical DDI, according to eq. 2 (Ito et al., 1998; Lau et al., 2007; CDER, 2012; Pan et al., 2013; Chioukh et al., 2014; Parvez et al., 2016):

$$\text{DDI index} = \frac{C_{\text{max}}}{\text{IC}_{50}} \text{ or } \frac{C_{\text{max,u}}}{\text{IC}_{50}} \quad (2)$$

**Quantification of T<sub>3</sub> by LC/MS/MS.** Cells were scraped and homogenized in 200 µl of water for T<sub>3</sub> analysis. Cell lysates were deproteinized by adding equal volumes of acetonitrile containing the internal standard. The mixture was vortexed and centrifuged at 15,000 × *g* for 5 minutes at room temperature. The supernatant was used directly for measurement. Chromatographic separation was performed using a Shimadzu Nexera high-performance liquid chromatography system (Shimadzu, Kyoto) with a Cosmosil 5C<sub>18</sub>-MS-II column (50 mm × 2.0 mm i.d., 5 µm; Nacalai Tesque).

To determine the T<sub>3</sub> concentration, the column was eluted with an isocratic flow of acetonitrile/water/acetic acid (30:70:0.1, v/v/v) at a flow rate of 0.2 ml/min. The injection volume was 5 µl, and the column temperature was maintained at 40°C. Positive and negative ion electrospray (ESI) tandem mass spectrometric analysis was performed using a TSQ Vantage EMR LC/MS/MS System (Thermo Scientific, Waltham, MA) at unit resolution with selected reaction monitoring. The transitions by selected reaction monitoring were *m/z* 652 > 606 for T<sub>3</sub> (ESI+) and *m/z* 423 > 101 for pravastatin (internal standard, ESI-). Data were acquired and analyzed using Xcalibur software (version 2.1; Thermo Scientific).

**Statistical Analysis.** Data are expressed as mean ± S.E. When appropriate, the differences between groups were tested for statistical significance using the unpaired Student's *t* test.  $P < 0.05$  was considered statistically significant.

## Results

**Establishment of OATP4C1 Stably Expressing Cells.** First, we tried to establish OATP4C1-expressing cells by use of human kidney-derived cell lines (HK-2, ACHN, HEK293, etc.); unfortunately, OATP4C1-expressed human cell lines could not be established. To examine the transport study of OATP4C1, we could establish a human OATP4C1-stably expressing cell system using canine renal tubule derived-MDCKII cells by following previous reports (Mikkaichi et al., 2004b; Yamaguchi et al., 2010). After selection with G418, single colonies for OATP4C1 expression were screened by transport studies.

First, we examined the transport of T<sub>3</sub>, which is a well-known substrate of OATP4C1. T<sub>3</sub> was statistically significantly transported by several OATP4C1-expressing clones, rather than by empty vector-transfected control cells. Because, among those clones, No. 68—hereafter referred to as OATP4C1/MDCKII cells—exhibited the highest OATP4C1 transport activity, we used this clone for the rest of the analysis.

We observed that sodium butyrate treatment statistically significantly enhanced OATP4C1-mediated T<sub>3</sub> uptake (Fig. 1A).

We adopted sodium butyrate treatment (5 mM, 24 hours) in reference to previous reports (Chen and Reith, 2007; Yang et al., 2009; Lu et al., 2013). We then tried to characterize the transport of  $T_3$  by OATP4C1 in the presence of sodium butyrate, and we observed that the time-dependent transport of  $T_3$  by the OATP4C1/MDCKII cells was statistically significantly higher than by the mock cells (Supplemental Fig. 1). After 60 minutes, the level of cellular accumulation of  $T_3$  in the OATP4C1/MDCKII cells ( $50 \pm 0.13$  pmol/mg protein) was 2.4-fold greater than in the mock cells ( $21 \pm 0.16$  pmol/mg protein). The apparent Michaelis-Menten constant ( $K_m$ ) for OATP4C1-mediated  $T_3$  uptake was  $7.9 \pm 1.3$   $\mu$ M in the presence of sodium butyrate (Supplemental Fig. 1). This value is comparable to the values previously reported by Mikkaichi et al. (2004b).

In addition, we confirmed the cell-surface expression of OATP4C1 in OATP4C1/MDCKII cells by Western blotting and immunohistochemical analyses. Western blotting showed the specific expression of OATP4C1 in OATP4C1/MDCKII cells (Fig. 1B). The protein expression amount was increased by exposure to sodium butyrate (Fig. 1, B and C). Furthermore, the immunohistochemical analysis showed the cell-surface expression of OATP4C1 in the cells exposed to sodium butyrate (Fig. 1D). Because more substrate was transported in the presence of

sodium butyrate, we decided to use cells exposed to it in all later experiments. Additionally, we performed our experiments within 40 passages, and the  $T_3$  uptake by OATP4C1/MDCKII cells was stable.

### Inhibitory Effects of Various Therapeutic Drugs on OATP4C1-Mediated Transport

To elucidate potential drug interactions via OATP4C1, we screened 53 representative drugs that are commonly used in clinical settings (Fig. 2). We selected and evaluated both renal and hepatic excretion drugs. Most of these drugs also have been reported to be transporter substrates or inhibitors, such as organic ion transporters and ABC transporters. Inhibitor concentrations were set much higher than those used in clinics (the solubility upper limit, or 100 times high) to avoid our overlooking the interaction.

OATP4C1-mediated transport was strongly inhibited (>50%) by 10 drugs: nicardipine (100  $\mu$ M), spironolactone (100  $\mu$ M), fluvastatin (50  $\mu$ M), crizotinib (50  $\mu$ M), levofloxacin (1000  $\mu$ M), clarithromycin (250  $\mu$ M), ritonavir (100  $\mu$ M), saquinavir (25  $\mu$ M), quinidine (100  $\mu$ M), and verapamil (100  $\mu$ M) (Fig. 2). Twelve other drugs also inhibited OATP4C1-mediated transport, but

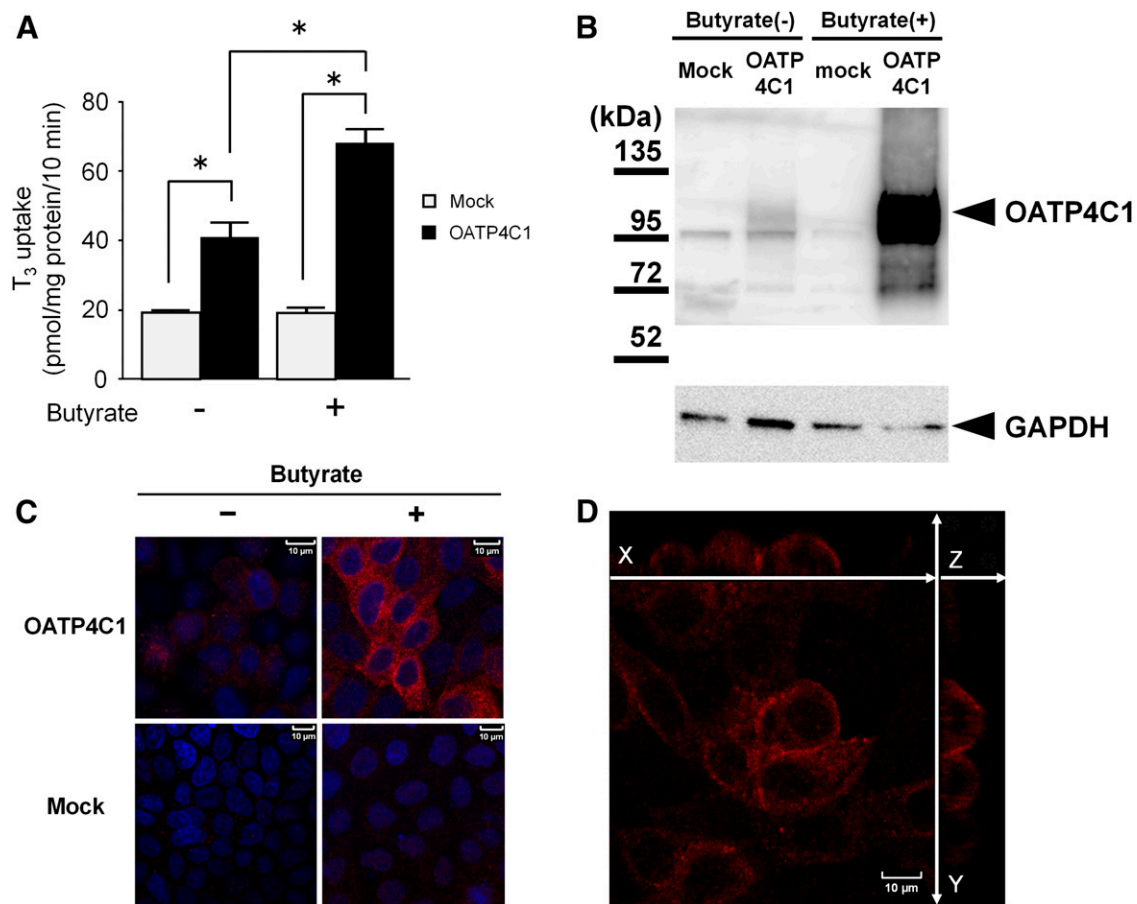


**Fig. 1.** Characterization of newly established OATP4C1-expressing MDCKII cells. (A) Samples were harvested 10 minutes after addition of  $T_3$  (1  $\mu$ M) to cells to monitor the level of  $T_3$  uptake. We compared the uptake of  $T_3$  into OATP4C1-expressing MDCKII cells with and without 5 mM sodium butyrate. The results are expressed as the mean  $\pm$  S.E. ( $n = 3$ ). \*Statistically significant difference from the value of the cells without 5 mM sodium butyrate ( $P < 0.05$ ). (B) Immunoblotting of OATP4C1 expressed in MDCKII cells with or without 5 mM sodium butyrate. The band at 95–135 kDa (arrowhead) represents OATP4C1. (C, D) Fluorescence microscopy of OATP4C1 expressed in MDCKII cells with or without 5 mM sodium butyrate. OATP4C1 proteins were observed in OATP4C1-transfected MDCKII cells (OATP4C1 proteins stained in red). Nuclei were stained with 4',6-diamidino-2-phenylindole (DAPI) in blue. Scale bars = 10  $\mu$ m. (D) OATP4C1 appears at the cell surface membrane in the presence of 5 mM sodium butyrate.

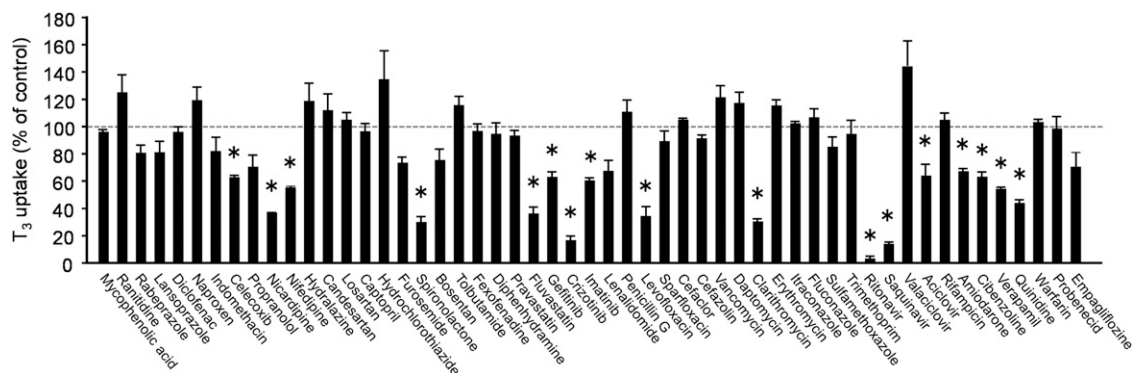


**Fig. 2.** Effects of various therapeutic drugs on  $T_3$  uptake by OATP4C1-expressing MDCKII cells. Cells were incubated for 10 minutes at 37°C with 1  $\mu\text{M}$   $T_3$  in the presence or absence of the trial drugs. Drug concentrations were as follows: 100  $\mu\text{M}$  mycophenolic acid, 100  $\mu\text{M}$  ranitidine, 100  $\mu\text{M}$  rabeprazole, 100  $\mu\text{M}$  lansoprazole, 100  $\mu\text{M}$  diclofenac, 100  $\mu\text{M}$  naproxen, 100  $\mu\text{M}$  indomethacin, 50  $\mu\text{M}$  celecoxib, 100  $\mu\text{M}$  propranolol, 100  $\mu\text{M}$  nicardipine, 100  $\mu\text{M}$  nifedipine, 100  $\mu\text{M}$  hydralazine, 100  $\mu\text{M}$  candesartan, 100  $\mu\text{M}$  losartan, 100  $\mu\text{M}$  captopril, 100  $\mu\text{M}$  hydrochlorothiazide, 100  $\mu\text{M}$  furosemide, 100  $\mu\text{M}$  spironolactone, 100  $\mu\text{M}$  bosentan, 100  $\mu\text{M}$  tolbutamide, 100  $\mu\text{M}$  fexofenadine, 100  $\mu\text{M}$  diphenhydramine, 50  $\mu\text{M}$  pravastatin, 50  $\mu\text{M}$  fluvastatin, 50  $\mu\text{M}$  gefitinib, 50  $\mu\text{M}$  crizotinib, 100  $\mu\text{M}$  imatinib, 100  $\mu\text{M}$  lenalidomide, 1000  $\mu\text{M}$  penicillin G, 1000  $\mu\text{M}$  levofloxacin, 100  $\mu\text{M}$  sparfloxacin, 100  $\mu\text{M}$  cefaclor, 1000  $\mu\text{M}$  cefazolin, 100  $\mu\text{M}$  vancomycin, 100  $\mu\text{M}$  daptomycin, 250  $\mu\text{M}$  clarithromycin, 100  $\mu\text{M}$  erythromycin, 25  $\mu\text{M}$  itraconazole, 1000  $\mu\text{M}$  fluconazole, 1000  $\mu\text{M}$  sulfamethoxazole, 100  $\mu\text{M}$  trimethoprim, 100  $\mu\text{M}$  ritonavir, 25  $\mu\text{M}$  saquinavir, 100  $\mu\text{M}$  valacyclovir, 1000  $\mu\text{M}$  acyclovir, 100  $\mu\text{M}$  rifampicin, 100  $\mu\text{M}$  amiodarone, 100  $\mu\text{M}$  cibenzoline, 100  $\mu\text{M}$  verapamil, 100  $\mu\text{M}$  quinidine, 100  $\mu\text{M}$  warfarin, 1000  $\mu\text{M}$  probenecid, and 100  $\mu\text{M}$  empagliflozin. OATP4C1-mediated transport was calculated after by taking the total cellular uptake by OATP4C1-expressing cells and subtracting the nonspecific uptake by mock cells. Each point and bar represents the mean  $\pm$  S.E. \*Statistically significant difference from the value of the drug-naïve cells ( $P < 0.05$ ).

the inhibition was moderate ( $>20\%$ ,  $<50\%$ ): celecoxib (50  $\mu\text{M}$ ), propranolol (100  $\mu\text{M}$ ), nifedipine (100  $\mu\text{M}$ ), furosemide (100  $\mu\text{M}$ ), bosentan (100  $\mu\text{M}$ ), gefitinib (50  $\mu\text{M}$ ), imatinib (100  $\mu\text{M}$ ), lenalidomide (100  $\mu\text{M}$ ), acyclovir (1000  $\mu\text{M}$ ), amiodarone (100  $\mu\text{M}$ ), cibenzoline (100  $\mu\text{M}$ ), and empagliflozin (100  $\mu\text{M}$ ) (Fig. 2). No statistically significant inhibition of OATP4C1-mediated transport was observed with the other 31 screened drugs (25–1000  $\mu\text{M}$ ) (Fig. 2).

Next, we evaluated the  $\text{IC}_{50}$  values of the 10 drugs that inhibited OATP4C1 by more than 50% (eq. 1, see *Materials and Methods*). All these drugs inhibited OATP4C1-mediated transport in a concentration-dependent manner (Fig. 3, A–J). The  $\text{IC}_{50}$  values of nicardipine, spironolactone, fluvastatin, crizotinib, levofloxacin, clarithromycin, ritonavir, saquinavir, quinidine, and verapamil for OATP4C1 were  $51 \pm 8$ ,  $53 \pm 7$ ,  $41 \pm 8$ ,  $24 \pm 8$ ,  $420 \pm 150$ ,  $200 \pm 16$ ,  $8.5 \pm 1.4$ ,  $4.3 \pm 0.6$ ,  $100 \pm 11$ , and  $110 \pm 22$   $\mu\text{M}$ , respectively.

**Prediction of the DDI Index.** To apply our results to clinical settings, we calculated the DDI indices according to the FDA guidelines using the maximum concentration in plasma ( $C_{\text{max}}$ ) and the unbound maximum concentration in plasma ( $C_{\text{max,u}}$ ) (eq. 2, see *Materials and Methods*). The DDI indices revealed that mild inhibition of OATP4C1-mediated uptake of typical substrates may occur even under normal conditions. When we estimated the inhibitory effects of ritonavir, quinidine, and saquinavir by using  $C_{\text{max}}$ , the DDI indices became significant (DDI index greater than the cutoff value of 0.1 suggested by regulatory authorities [i.e., FDA]) whereas levofloxacin, clarithromycin, crizotinib, spironolactone, fluvastatin, nicardipine, and verapamil showed negligible DDI indices (Table 1).

The maximum DDI indices of ritonavir, quinidine, and saquinavir were 1.9, 0.86, and 0.19 for OATP4C1-mediated  $T_3$  uptake inhibition (Table 1). The calculated maximum DDI indices of levofloxacin, clarithromycin, crizotinib, spironolactone, fluvastatin, nicardipine, and verapamil were 0.045, 0.019, 0.046, 0.0091, 0.016, 0.0053, and 0.0046, respectively, for OATP4C1-mediated  $T_3$  uptake inhibition (Table 1). Among the tested drugs,

ritonavir showed the highest DDI index for OATP4C1, indicating a strong possibility of clinical drug interactions.

## Discussion

Several studies have revealed the impacts of metabolism mediated by cytochrome P450 isoform 3A (CYP3A) and of renal excretion mediated by OAT and P-glycoprotein (P-gp) on the pharmacokinetic alteration of drugs (Laskin et al., 1982; Vree et al., 1995; Hsu et al., 1998; Ouellet et al., 1998; Landersdorfer et al., 2010; Schmitt et al., 2010); however, other processes such as transcellular dynamics regulated by other transporters cannot be ignored. OCT and MATE have been also evaluated in several studies (Yonezawa and Inui, 2011). OATP4C1 is one of transporters whose interactions have remained unknown.

In our present study, we evaluated the interactions of various therapeutic drugs with the kidney-specific organic anion transporter OATP4C1. This is the first report to clarify and summarize the interactions of therapeutic drugs on OATP4C1-mediated transport. Although we evaluated OATP4C1-mediated  $T_3$  uptake in the presence of sodium butyrate, the transport characteristics of  $T_3$  by OATP4C1 were comparable with those found in a previous report that did not use sodium butyrate (Mikkaichi et al., 2004b). Further, we confirmed OATP4C1-expression in MDCKII cells by performing Western blot and immunohistochemical analyses. Our results show that OATP4C1 may be a drug transporter implicated in DDIs in clinical settings. This novel finding could provide essential information for drug therapy and drug development in the future.

From the screening results, we found that OATP4C1-mediated  $T_3$  transport was inhibited by 22 out of 53 therapeutic drugs (Fig. 2). Among these drugs, the inhibitory effects of 10 drugs on OATP4C1-mediated transport were strong ( $>50\%$ ) (Fig. 2). These 10 drugs include many drugs that have been reported to be substrates or inhibitors of other drug transporters such as hepatic OATPs, organic ion transporters, and ABC transporters in the kidney (Supplemental Table 1). Another 12 drugs also inhibited OATP4C1-mediated transport, but the inhibition by

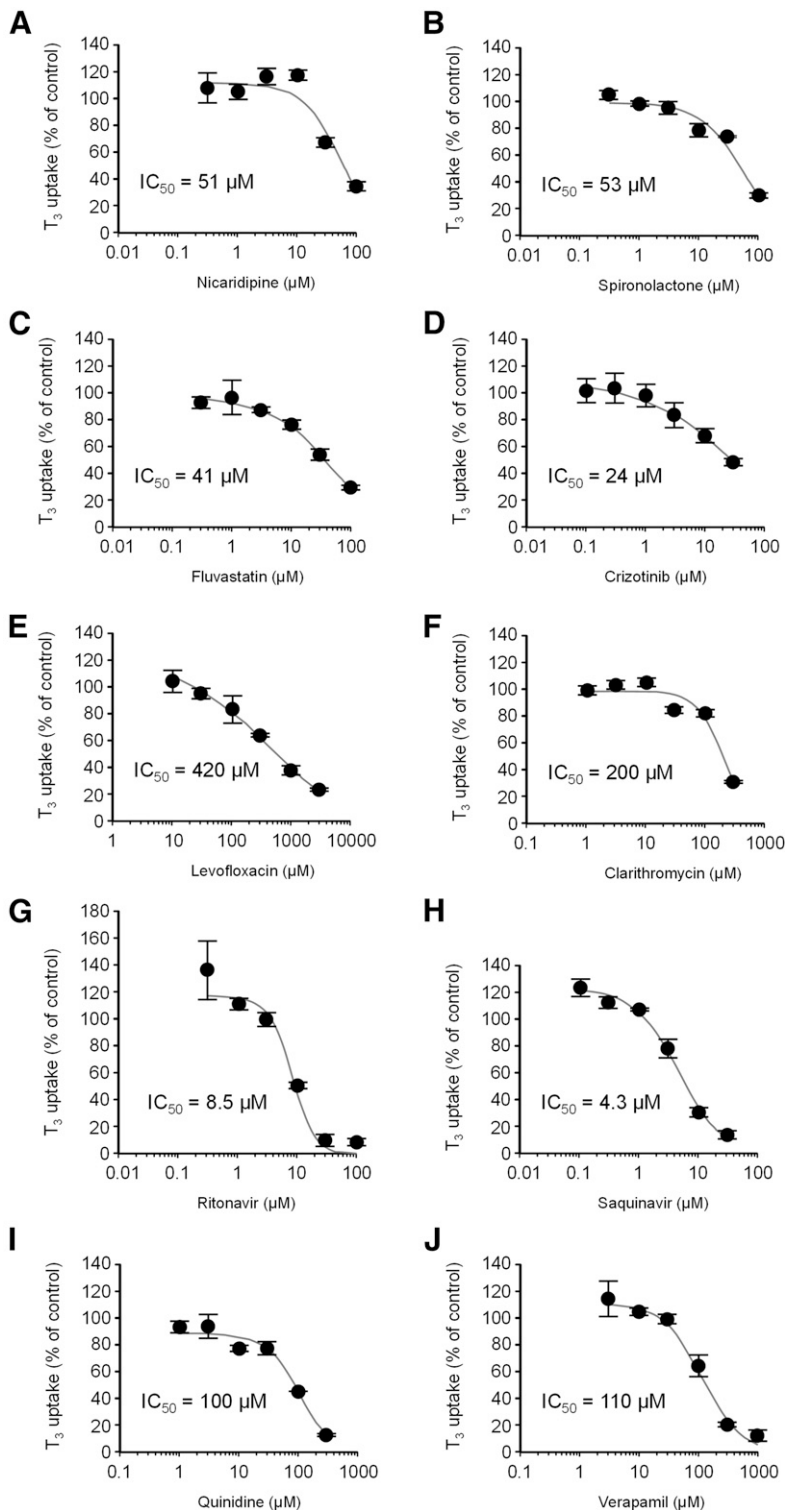


**Fig. 3.** Inhibitory effects of 10 drugs on OATP4C1-mediated  $T_3$  uptake. Cells were incubated for 10 minutes at  $37^\circ\text{C}$  with  $1\ \mu\text{M}$   $T_3$  in the presence or absence of (A) nicardipine ( $0.3\text{--}100\ \mu\text{M}$ ), (B) spironolactone ( $0.3\text{--}100\ \mu\text{M}$ ), (C) fluvastatin ( $0.3\text{--}100\ \mu\text{M}$ ), (D) crizotinib ( $0.1\text{--}30\ \mu\text{M}$ ), (E) levofloxacin ( $10\text{--}3000\ \mu\text{M}$ ), (F) clarithromycin ( $1\text{--}300\ \mu\text{M}$ ), (G) ritonavir ( $0.3\text{--}100\ \mu\text{M}$ ), (H) saquinavir ( $0.1\text{--}30\ \mu\text{M}$ ), (I) quinidine ( $1\text{--}300\ \mu\text{M}$ ), or (J) verapamil ( $3\text{--}1000\ \mu\text{M}$ ). OATP4C1-mediated transport was calculated after by taking the total cellular uptake by OATP4C1-expressing cells and subtracting the nonspecific uptake by mock cells. Each point and bar represents the mean  $\pm$  S.E. The data are shown as a percentage of the transport done by the control. Solid lines represent fitted lines for the inhibition of  $T_3$  uptake by the inhibitors that were obtained by a nonlinear least-squares regression analysis based on eq. 1.

those drugs was moderate ( $>20\%$   $<50\%$ ) (Fig. 2). As our previous study showed that OATP4C1 has multiple binding sites for its substrate (Yamaguchi et al., 2010), if other OATP4C1 substrates besides  $T_3$  had been used in the drug screening different results may have been observed. Estrone 3-sulfate and digoxin are also reported to be substrates of OATP4C1 (Mikkaichi et al., 2004b; Yamaguchi et al., 2010).

We also found in this study that these compounds were transported by established OATP4C1/MDCKII cells. However,

OATP4C1-mediated estrone 3-sulfate and digoxin uptake is less than OATP4C1-mediated  $T_3$  transport, and it was difficult to evaluate the inhibition of therapeutic drugs by using those substrates. Further study is needed to obtain more information about OATP4C1 interactions with therapeutic drugs.

Next, we evaluated the  $\text{IC}_{50}$  values of the 10 drugs that showed strong inhibition, all of which inhibited OATP4C1-mediated transport in a concentration-dependent manner (Fig. 3, A–J). The  $\text{IC}_{50}$  values of nicardipine, spironolactone,

TABLE 1

Drug-drug interaction (DDI) indices estimated from *in vitro* OATP4C1-mediated  $T_3$  uptake inhibition kinetics by therapeutic drugs

$IC_{50}$  ( $\mu\text{M}$ ) are shown as mean  $\pm$  S.E., and  $f_{\text{max,u}}$  (%) is the unbound fraction of the drugs. Data for  $C_{\text{max}}$  and  $f_{\text{max,u}}$  (%) of the drugs are taken from previous reports. The DDI indices were determined using the inhibition constant ( $IC_{50}$ ) with the maximum plasma concentration ( $C_{\text{max}}$ ; bound plus unbound) ( $I|_{\text{max}}$ ) and the maximum unbound concentration ( $C_{\text{max,u}}$ ) ( $I|_{\text{max,u}}$ ) of the drugs following the regulatory guidelines described in the text.

Drug	$IC_{50}$ ( $\mu\text{M}$ )	$C_{\text{max}}$ ( $\mu\text{M}$ )	$C_{\text{max,u}}$ ( $\mu\text{M}$ )	$f_{\text{max,u}}$ (%)	DDI index	
					$I  = I _{\text{max}}$	$I  = I _{\text{max,u}}$
Levofloxacin	420 $\pm$ 150	19 <sup>a</sup>	14.1	74 <sup>a</sup>	0.045	0.033
Ritonavir	8.5 $\pm$ 1.4	16 <sup>b</sup>	0.16	1 <sup>b</sup>	1.9	0.019
Quinidine	100 $\pm$ 11	19 <sup>c</sup>	1.9	10 <sup>c</sup>	0.19	0.019
Saquinavir	4.3 $\pm$ 0.6	3.7 <sup>b</sup>	0.074	2 <sup>b</sup>	0.86	0.0172
Clarithromycin	200 $\pm$ 16	3.8 <sup>d</sup>	1.9	50 <sup>d</sup>	0.019	0.0095
Crizotinib	24 $\pm$ 8	1.1 <sup>e</sup>	0.099	9 <sup>e</sup>	0.046	0.0041
Spirolactone	53 $\pm$ 7	0.48 <sup>f</sup>	0.048	10 <sup>f</sup>	0.0091	0.00091
Fluvastatin	41 $\pm$ 8	0.65 <sup>g</sup>	0.033	5 <sup>g</sup>	0.016	0.00079
Nicardipine	51 $\pm$ 8	0.27 <sup>h</sup>	0.027	10 <sup>h</sup>	0.0053	0.00053
Verapamil	110 $\pm$ 22	0.51 <sup>i</sup>	0.051	10 <sup>i</sup>	0.0046	0.00046

<sup>a</sup>Values obtained from Rodvold and Neuhauser (2001).

<sup>b</sup>Values obtained from Hsu et al. (1998).

<sup>c</sup>Values obtained from Capucci et al. (1998).

<sup>d</sup>Values obtained from Rodvold (1999).

<sup>e</sup>Values obtained from Fujiwara et al. (2016).

<sup>f</sup>Values obtained from Overdiek et al. (1985).

<sup>g</sup>Values obtained from Scripture and Pieper (2001).

<sup>h</sup>Values obtained from Forette et al. (1985).

<sup>i</sup>Values obtained from Krecic-Shepard et al. (2000).

fluvastatin, crizotinib, levofloxacin, clarithromycin, ritonavir, saquinavir, quinidine, and verapamil obtained in this study were 51, 53, 41, 24, 420, 200, 8.5, 4.3, 100, and 110  $\mu\text{M}$ , respectively. The  $IC_{50}$  values of these drugs were higher than the plasma concentrations obtained in clinical practice (Table 1). Additionally, the  $IC_{50}$  values of clarithromycin, levofloxacin, nicardipine, and quinidine were higher than those of hepatic OATPs, organic ion transporters, and ABC transporters expressed in proximal tubular cells (Supplemental Table 1). Crizotinib, fluvastatin, ritonavir, saquinavir, and verapamil showed equivalent or higher affinity to OATP4C1 than to those transporters located in the liver and kidney (Supplemental Table 1).

Additionally, we estimated the DDI indices and applied our results to clinical settings according to the FDA guidelines. As expected, the DDI indices of those drugs were not significant (DDI index  $<0.1$ ) under normal conditions. However, when we estimated the inhibitory effects of ritonavir, quinidine, and saquinavir by using  $C_{\text{max}}$ , the DDI indices were significant (DDI index  $>0.1$ ) whereas levofloxacin, clarithromycin, crizotinib, spiro lactone, fluvastatin, nicardipine, and verapamil showed negligible DDI indices. When we estimated the effect of the drugs on drug transporters, the fraction that was not protein-bound had to be taken into consideration. Among the drugs evaluated in this study, many are more than 90% protein-bound in plasma (Table 1). Thus, the effects of those drugs on OATP4C1 are thought to be small under normal conditions.

However, in chronic disease states, such as chronic hepatic dysfunction and CKD, the DDI indices of drugs should be higher because of an increased proportion of unbound drugs. Furthermore, patients with chronic hepatic dysfunction or CKD frequently have hypoalbuminemia, which also results in an increase in protein-unbound drugs (Viani et al., 1989; Meijers et al., 2008). It has also been reported that, compared with control subjects, dialysis patients have significantly lower levels of albumin (Małgorzewicz et al., 2008).

For example, the plasma concentration of fluvastatin is reported to be increased in patients with hepatic dysfunction

compared with healthy subjects ( $C_{\text{max}}$  683  $\mu\text{g/l}$  [1.7  $\mu\text{M}$ ] versus 269  $\mu\text{g/l}$  [0.65  $\mu\text{M}$ ]) (Scripture and Pieper, 2001). In addition, the plasma albumin concentration is reported to decrease to 3.2 g/dl (cirrhosis) and 2.3 g/dl (sepsis) (versus healthy 4.8 g/dl) (Oetl et al., 2013). It could be simply estimated that  $C_{\text{max,u}}$  of fluvastatin increases to  $C_{\text{max}}$ , which is shown in Table 1. Further, high bilirubin concentrations in patients with cirrhosis could increase unbound drug concentration because bilirubin is also has high affinity to albumin (Oetl et al., 2013).

Although no previous reports exist that mention free drug concentrations in renal tubular lumen under pathologic conditions, we simply discussed the necessity of drug adjustment by referring to important information such as hypoalbuminemia in pathologic condition and lower levels of albumin in dialysis patients. We could estimate the inhibitory effects of drugs on OATP4C1 by using the  $IC_{50}$  values and DDI indices in patients with chronic disease states. Among the tested drugs, ritonavir showed the highest DDI index for OATP4C1 under low albumin conditions, indicating a strong possibility of clinical drug interactions in patients with chronic disease states.

Previous studies of ritonavir have suggested that significant interactions could occur with drugs that are extensively metabolized by CYP3A (Hsu et al., 1998). For example, ritonavir increased the area under the curve of clarithromycin by 77% (Ouellet et al., 1998). Additionally, ritonavir almost completely inhibited the formation of 14-hydroxy-clarithromycin, which is formed by the metabolic enzyme CYP3A (Ouellet et al., 1998).

Although several studies have revealed the impact of CYP3A-mediated metabolism on the pharmacokinetic alteration of drugs, other processes such as transcellular dynamics regulated by several transporters cannot be ignored. Ritonavir has been reported to have a high affinity for P-gp (Vermeer et al., 2016). Clinically, it was reported that pretreatment with saquinavir/ritonavir at 1000/100 mg twice daily increased digoxin exposure, most likely via P-gp inhibition (Schmitt et al., 2010). Although previous reports have stated that CYP3A and P-gp were the most likely molecules responsible for the altered drug pharmacokinetics,

those molecules cannot explain the whole of the drug interactions *in vivo*. Ritonavir showed the strongest interaction with OATP4C1 in our study. Out of 53 drugs tested, only 3 (i.e., 5%)—ritonavir, quinidine, and saquinavir—had DDI indices ( $C_{\max}/IC_{50}$ ) > 0.1. Our result is similar to that reported for OAT1 (35/727 compounds [5%]) and OAT3 (73/727 compounds [10%]) (Duan et al., 2012). In addition, these three drugs have all been shown to exhibit renal DDI with digoxin, supporting a recent proposal from physiologically based pharmacokinetic modeling that uptake is rate limiting in digoxin renal excretion (Scotcher et al., 2017).

It is possible that OATP4C1 plays an important role in the drug interactions discussed here. Further study is needed to clarify the contribution of OATP4C1 to the well-known drug interactions seen in clinical practice. We have provided novel information about OATP4C1-based interactions between various therapeutic drugs. We also evaluated the possibility of OATP4C1 involvement in DDIs by using the  $IC_{50}$  values and DDI indices. OATP4C1 may have an important role in clinical therapy, and our findings provide new insight into investigations of DDI and drug development in the future.

#### Authorship Contributions

*Participated in research design:* Sato, Abe, Yamaguchi.

*Conducted experiments:* Sato, Mishima, Yamaguchi.

*Performed data analysis:* Sato, Mishima, Yamaguchi.

*Wrote or contributed to the writing of the manuscript:* Sato, Mishima, Mano, Abe, Yamaguchi.

#### References

- Capucci A, Aschieri D, and Villani GQ (1998) Clinical pharmacology of antiarrhythmic drugs. *Drugs Aging* **13**:51–70.
- Chen N and Reith ME (2007) Substrates and inhibitors display different sensitivity to expression level of the dopamine transporter in heterologously expressing cells. *J Neurochem* **101**:377–388.
- Chioukh R, Noel-Hudson MS, Ribes S, Fournier N, Becquemont L, and Verstuyft C (2014) Proton pump inhibitors inhibit methotrexate transport by renal basolateral organic anion transporter hOAT3. *Drug Metab Dispos* **42**:2041–2048.
- Chu XY, Bleasby K, Yabut J, Cai X, Chan GH, Hafey MJ, Xu S, Bergman AJ, Braun MP, Dean DC, et al. (2007) Transport of the dipeptidyl peptidase-4 inhibitor sitagliptin by human organic anion transporter 3, organic anion transporting polypeptide 4C1, and multidrug resistance P-glycoprotein. *J Pharmacol Exp Ther* **321**:673–683.
- Duan P, Li S, Ai N, Hu L, Welsh WJ, and You G (2012) Potent inhibitors of human organic anion transporters 1 and 3 from clinical drug libraries: discovery and molecular characterization. *Mol Pharm* **9**:3340–3346.
- Center for Drug Evaluation and Research (CDER) (2012) *Guidance for Industry: Drug Interaction Studies—Study Design, Data Analysis, Implications for Dosing, and Labeling Recommendations* U.S. Department of Health and Human Services, Food and Drug Administration, Rockville, MD.
- Forette F, Bellet M, Henry JF, Hervy MP, Poyard-Salmeron C, Bouchacourt P, and Guerret M (1985) Effect of nicardipine in elderly hypertensive patients. *Br J Clin Pharmacol* **20** (Suppl 1):125S–129S.
- Fujiwara Y, Hamada A, Mizugaki H, Aikawa H, Hata T, Horinouchi H, Kanda S, Goto Y, Itahashi K, Nohihara H, et al. (2016) Pharmacokinetic profiles of significant adverse events with crizotinib in Japanese patients with ABCB1 polymorphism. *Cancer Sci* **107**:1117–1123.
- Hagenbuch B and Meier PJ (2003) The superfamily of organic anion transporting polypeptides. *Biochim Biophys Acta* **1609**:1–18.
- Hagenbuch B and Meier PJ (2004) Organic anion transporting polypeptides of the OATP/SLC21 family: phylogenetic classification as OATP/SLCO superfamily, new nomenclature and molecular/functional properties. *Pflugers Arch* **447**:653–665.
- Hsu A, Granneman GR, and Bertz RJ (1998) Ritonavir. Clinical pharmacokinetics and interactions with other anti-HIV agents. *Clin Pharmacokinet* **35**:275–291.
- Ito K, Iwatsubo T, Kanamitsu S, Ueda K, Suzuki H, and Sugiyama Y (1998) Prediction of pharmacokinetic alterations caused by drug-drug interactions: metabolic interaction in the liver. *Pharmacol Rev* **50**:387–412.
- Izumi S, Nozaki Y, Maeda K, Komori T, Takenaka O, Kusuhara H, and Sugiyama Y (2015) Investigation of the impact of substrate selection on *in vitro* organic anion transporting polypeptide 1B1 inhibition profiles for the prediction of drug-drug interactions. *Drug Metab Dispos* **43**:235–247.
- Krecic-Shepard ME, Barnas CR, Slimko J, Jones MP, and Schwartz JB (2000) Gender-specific effects on verapamil pharmacokinetics and pharmacodynamics in humans. *J Clin Pharmacol* **40**:219–230.
- Kullak-Ublick GA, Stieger B, and Meier PJ (2004) Enterohepatic bile salt transporters in normal physiology and liver disease. *Gastroenterology* **126**:322–342.
- Landersdorfer CB, Kirkpatrick CM, Kinzig M, Bulitta JB, Holzgrabe U, Jaehde U, Reiter A, Naber KG, Rodamer M, and Sörgel F (2010) Competitive inhibition of renal tubular secretion of ciprofloxacin and metabolite by probenecid. *Br J Clin Pharmacol* **69**:167–178.
- Laskin OL, de Miranda P, King DH, Page DA, Longstreth JA, Rocco L, and Lietman PS (1982) Effects of probenecid on the pharmacokinetics and elimination of acyclovir in humans. *Antimicrob Agents Chemother* **21**:804–807.
- Lau YY, Huang Y, Frassetto L, and Benet LZ (2007) Effect of OATP1B transporter inhibition on the pharmacokinetics of atorvastatin in healthy volunteers. *Clin Pharmacol Ther* **81**:194–204.
- Lu Y, Nakanishi T, and Tamai I (2013) Functional cooperation of SMCTs and URAT1 for renal reabsorption transport of urate. *Drug Metab Pharmacokinet* **28**:153–158.
- Malgorzewicz S, Debska-Slizien A, Rutkowski B, and Lysiak-Szydłowska W (2008) Serum concentration of amino acids versus nutritional status in hemodialysis patients. *J Ren Nutr* **18**:239–247.
- Meijers BK, Bammens B, Verbeke K, and Evenepoel P (2008) A review of albumin binding in CKD. *Am J Kidney Dis* **51**:839–850.
- Mikkaichi T, Suzuki T, Tanemoto M, Ito S, and Abe T (2004a) The organic anion transporter (OATP) family. *Drug Metab Pharmacokinet* **19**:171–179.
- Mikkaichi T, Suzuki T, Onogawa T, Tanemoto M, Mizutamari H, Okada M, Chaki T, Masuda S, Tokui T, Eto N, et al. (2004b) Isolation and characterization of a digoxin transporter and its rat homologue expressed in the kidney. *Proc Natl Acad Sci USA* **101**:3569–3574.
- Oettl K, Birner-Gruenberger R, Spindelboeck W, Stueger HP, Dorn L, Stadlbauer V, Putz-Bankuti C, Krisper P, Graziadei I, Vogel W, et al. (2013) Oxidative albumin damage in chronic liver failure: relation to albumin binding capacity, liver dysfunction and survival. *J Hepatol* **59**:978–983.
- Ouellet D, Hsu A, Granneman GR, Carlson G, Cavanaugh J, Guenther H, and Leonard JM (1998) Pharmacokinetic interaction between ritonavir and clarithromycin. *Clin Pharmacol Ther* **64**:355–362.
- Overdiek HW, Hermens WA, and Merkus FW (1985) New insights into the pharmacokinetics of spironolactone. *Clin Pharmacol Ther* **38**:469–474.
- Pan X, Wang L, Gründemann D, and Sweet DH (2012) Interaction of Ethambutol with human organic cation transporters of the SLC22 family indicates potential for drug-drug interactions during antituberculosis therapy. *Antimicrob Agents Chemother* **57**:5053–5059.
- Parvez MM, Kaiser N, Shin HJ, Jung JA, and Shin JG (2016) Inhibitory interaction potential of 22 antituberculosis drugs on organic anion and cation transporters of the SLC22A family. *Antimicrob Agents Chemother* **60**:6558–6567.
- Rodvold KA (1999) Clinical pharmacokinetics of clarithromycin. *Clin Pharmacokinet* **37**:385–398.
- Rodvold KA and Neuhauser M (2001) Pharmacokinetics and pharmacodynamics of fluoroquinolones. *Pharmacotherapy* **21**:233S–252S.
- Sato T, Yamaguchi H, Kogawa T, Abe T, and Mano N (2014) Organic anion transporting polypeptides 1B1 and 1B3 play an important role in uremic toxin handling and drug-uremic toxin interactions in the liver. *J Pharm Pharm Sci* **17**:475–484.
- Sato T, Ito H, Hirata A, Abe T, Mano N, and Yamaguchi H (2017) Interactions of crizotinib and gefitinib with organic anion-transporting polypeptides (OATP)1B1, OATP1B3 and OATP2B1: gefitinib shows contradictory interaction with OATP1B3. *Xenobiotica* DOI: 10.1080/00498254.2016.1275880 [published ahead of print].
- Schmitt C, Kaeser B, Riek M, Bech N, and Kreuzer C (2010) Effect of saquinavir/ritonavir on P-glycoprotein activity in healthy volunteers using digoxin as a probe. *Int J Clin Pharmacol Ther* **48**:192–199.
- Scotcher D, Jones CR, Galetin A, and Rostami-Hodjegan A (2017) Delineating the role of various factors in renal disposition of digoxin through application of physiologically based kidney model to renal impairment populations. *J Pharmacol Exp Ther* **360**:484–495.
- Scripture CD and Pieper JA (2001) Clinical pharmacokinetics of fluvastatin. *Clin Pharmacokinet* **40**:263–281.
- Suga T, Yamaguchi H, Sato T, Maekawa M, Goto J, and Mano N (2017) Preference of conjugated bile acids over unconjugated bile acids as substrates for OATP1B1 and OATP1B3. *PLoS One* **12**:e0169719.
- Toyohara T, Suzuki T, Morimoto R, Akiyama Y, Souma T, Shiwaku HO, Takeuchi Y, Mishima E, Abe M, Tanemoto M, et al. (2009) SLC04C1 transporter eliminates uremic toxins and attenuates hypertension and renal inflammation. *J Am Soc Nephrol* **20**:2546–2555.
- Vermeer LM, Istringhausen CD, Ogilvie BW, and Buckley DB (2016) Evaluation of ketoconazole and its alternative clinical CYP3A4/5 inhibitors as inhibitors of drug transporters: the *in vitro* effects of ketoconazole, ritonavir, clarithromycin, and itraconazole on 13 clinically-relevant drug transporters. *Drug Metab Dispos* **44**:453–459.
- Viani A, Carrai M, and Pacifici GM (1989) Plasma protein binding of frusemide in liver disease: effect of hypoalbuminaemia and hyperbilirubinaemia. *Br J Clin Pharmacol* **28**:175–178.
- Vree TB, van den Biggelaar-Marteau M, and Verwey-van Wissen CP (1995) Probenecid inhibits the renal clearance of frusemide and its acyl glucuronide. *Br J Clin Pharmacol* **39**:692–695.
- Yamaguchi H, Sugie M, Okada M, Mikkaichi T, Toyohara T, Abe T, Goto J, Hishinuma T, Shimada M, and Mano N (2010) Transport of estrone 3-sulfate mediated by organic anion transporter OATP4C1: estrone 3-sulfate binds to the different recognition site for digoxin in OATP4C1. *Drug Metab Pharmacokinet* **25**:314–317.
- Yang CH, Glover KP, and Han X (2009) Organic anion transporting polypeptide (Oatp) 1a1-mediated perfluorooctanoate transport and evidence for a renal reabsorption mechanism of Oatp1a1 in renal elimination of perfluorocarboxylates in rats. *Toxicol Lett* **190**:163–171.
- Yonezawa A and Inui K (2011) Organic cation transporter OCT/SLC22A and H(+)/organic cation antiporter MATE/SLC47A are key molecules for nephrotoxicity of platinum agents. *Biochem Pharmacol* **81**:563–568.

**Address correspondence to:** Dr. Hiroaki Yamaguchi, Department of Pharmaceutical Sciences, Tohoku University Hospital, 1-1 Seiryomachi, Aoba-ku, Sendai 980-8574, Japan. E-mail: yamaguchi@hosp.tohoku.ac.jp